MECHANICAL LOADING, SEX, AGE, AND CORTICAL LOCATION INFLUENCE BONE TISSUE COMPOSITION IN MICE

Honors Thesis

Presented to the College of Agriculture and Life Sciences, Biological Sciences

of Cornell University

in Partial Fulfillment of the Requirements for the

Research Honors Program

by

Daniel Joseph Walsh

May 2009

Professor Marjolein van der Meulen

À Pepe

Même si tu as quitté ce monde, je porte en moi ton courage et je souris.

Acknowledgments

This research was supported by NIH grant AG028664 and grants from the College of Agriculture and Life Sciences and the Department of Biological Sciences at Cornell University.

I would like to thank Maureen Lynch, Grace Kim, and Jayme Burket for their assistance, knowledge, and support throughout this project.

Many thanks to Dr. Russell Main for his mentorship and guidance over the past two years.

I would also like to thank the entire van der Meulen research group and the Biomechanics Department.

Special thanks to Dr. Adele Boskey, Dr. Eve Donnelly, and Dr. Christopher Umbach for their guidance on Raman spectroscopy.

I want to thank my family for their love, encouragement, and support throughout my life.

Many thanks to my friends. I will never forget our time on the Hill.

Finally, I would like to thank Dr. Marjolein van der Meulen. None of this would have been possible without her. I am grateful for the opportunities and high standards she has given me. The opportunity to learn and work in her lab has been my greatest academic experience at Cornell.

Table of Contents

List of Figures

Abstract

The application of non-invasive mechanical loads to rodent limbs induces geometric and material changes in the skeleton[11]. Geometric adaptation has been characterized extensively, but the material changes are less well understood. Raman microspectroscopy measures chemical composition at the tissue level and was used to determine the effects of *in vivo* mechanical loading, sex, age, and cortical location on periosteal composition in mouse tibiae. The degree of mineralization (mineral-to-matrix) and carbonate substitution (CO_3^{2-}:PO_4^{3-}) ratios were used to assess tissue composition. The degree of mineralization at the periosteum was lower with loading in all mouse groups. Sex and age-based differences in mineralization were present in the control limbs. Males had greater mineralization but lower carbonate substitution than females. Mature females were more mineralized than but had similar carbonate substitution to younger growing females. Variation in tissue composition by cortical location occurred in mature females but not in growing females and males. To understand the implications of these findings on functional performance, the material changes reported here need to be combined with geometric and morphological analyses to form a more complete view of structural adaptation of the tibia.

Introduction

Bone is a dynamic organ with a diverse range of forms, functions, and properties. In its role in the skeleton, bone provides structural support for motion, physical load bearing, internal organ protection, and calcium storage. Failure to meet these demands reduces skeletal integrity and can result in fracturing and serious injury. Bone has unique geometric and material properties which contribute to whole bone functional performance and integrity. Neither geometry nor material can be solely used to fully determine skeletal performance and integrity[26]. The relationship between geometric and material properties is not fully understood and relating them has been a challenge in bone research. To address this challenge, animal models are widely used to test and analyze the geometric and material properties of bone.

The ability of a whole bone to bear functional loads depends on both its geometric and material properties. In mouse tibiae, mechanical loading increases mineral content and bone mass in a loaded relative to a contralateral control limb. Mechanically loaded limbs show appreciable geometric differences from control limbs[11] (Fig. 1).

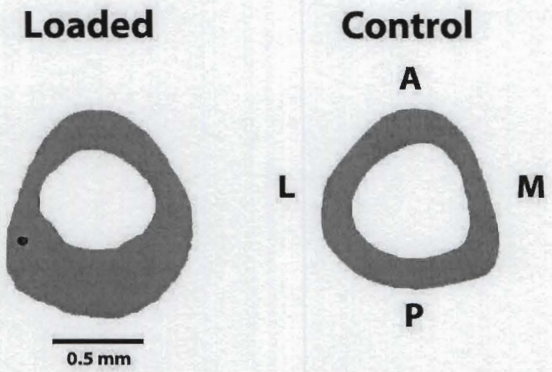

Figure 11. Representational image of the effect of 2 weeks of *in vivo* mechanical loading on bone geometry in 10 week old C57BL/6J female mouse tibiae. Left (loaded) and right (control) cross sectional images were taken at the mid-diaphysis. The loaded limb shows an increased cross sectional geometry relative to the control limb among the anterior (A), lateral (L), medial (M), and posterior (P) quadrants. [From R. Main et al., 2008, ORS][13].

Geometrical adaptation to mechanical loads is part of whole bone adaptation which involves the active gain or loss of bone tissue. Cross sectional area, area moment of inertia, and bone length are geometric properties that influence the mechanical behavior of bone and are altered over time by mechanical loading[4,11,27]. Bones with large cross sectional areas and area moments of inertia are stronger and stiffer than bones with smaller areas assuming the bone materials are identical. Long bones have higher bending moments and thus higher magnitudes of stress (force/area) than short bones. If all else is equal, failure under loading (structural strength) will occur sooner in longer than in shorter bones. The size and shape (distribution of material) determine these geometric properties and influence structural performance.

Geometric properties alone cannot determine whole bone structural performance or failure under loading. Material properties such as stress, strain (deformation), and the elastic modulus (stress/strain) dictate a bone's resistance to deformation (stiffness) and other whole bone structural properties. At the material level, mineral composition, collagen content and orientation, mineral density, crystal size, and overall structural organization influence the material behavior[3]. In a load-deformation (stress-strain) curve of bone, the steeper the slope of the elastic modulus, indicated by the initial linear region, the stiffer the material[14] (Fig. 2).

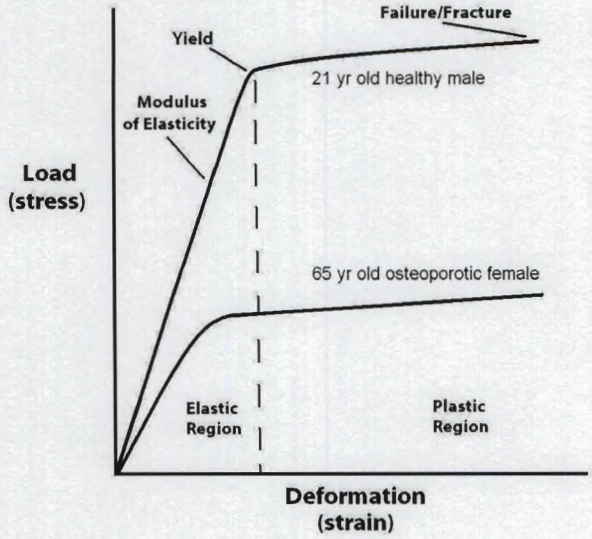

Figure 12. Load-deformation curve for vertebrae bone tissue. Curves represent the stress-strain relationship for 21 year old healthy male vertebrae and 65 year old osteoporotic female vertebrae. The stiffness (modulus of elasticity) is greater in the male vertebrae than in the female vertebrae. [Adapted from P. Thurner et al. 2005, Mater. Res. Soc. Symp. Proc. Vol. 874, 2005][24].

Many studies have used mechanical testing to report the geometric and material properties of bone such as area moment of inertia and elastic modulus, respectively[1,4,8, 11,12,20]. Few studies have reported compositional changes and their relationship to properties such as area moment of inertia and elastic modulus[1]. Compositional changes due to mechanical loading have never been reported, yet this information is necessary to understand the implications of mechanical stimuli on material properties and structural performance.

Bone tissue consists of organic and inorganic phases. Over 90% of the organic matrix is type I collagen, a 300 nm protein fiber, which in a cross-linking pattern with other collagen fibers, contributes to mechanical properties such as elasticity and tensile strength[27]. Noncollagenous proteins and other macromolecules make up the remaining 10%. Calcium phosphate (crystalline calcium hydroxyapatite) is the principal mineral

component of the inorganic phase. Ions such as carbonate (CO_3^{2-}) and fluoride (F^-) can substitute for phosphate but the physical properties of hydroxyapatite such as solubility and crystal size change as a result and alter the crystal's normal function. Carbonate substitution, for example, creates structural defects and lowers crystallinity in the hydroxyapatite lattice[19]. How compositional changes like carbonate substitution affect whole bone function is not fully understood, although studies have shown a relationship between increased mineralization and substitution and impaired elasticity in rats and humans[1, 2]. To characterize compositional changes, spectroscopic techniques have been widely used.

Spectroscopy, which is the interaction between electromagnetic radiation and matter, incorporates a broad range of techniques and provides chemical and structural information about a material. The fundamental principle behind spectroscopy states that molecules undergo quantized energy transitions after photon absorption or emission. The change in energy (ΔE) after absorption or emission is proportional to the frequency (ν/s^{-1}) of the incoming/outgoing light.

$$\Delta E = E_2 - E_1 = h\nu$$

E_1 and E_2 are different quantized energy levels and h is Planck's constant. Graphically, a spectral line represents the energy change (band shift) between two states denoted on the x-axis by wavenumber ($\ddot{\upsilon}/cm^{-1}$), or inverse wavelength (λ^{-1}).

$$\ddot{\upsilon} = 1/\lambda = \nu/c \quad \text{where c=speed of light}$$

The height or intensity of the spectra band is related to the number of molecules involved in the transition from E_1 to E_2 and is denoted on the y-axis (unitless)[7]. Molecular species have different chemistry and bonding arrangements and are distinguishable by their

spectra which allow chemical identification and comparison among proteins, crystals, and other chemical species (Fig.3).

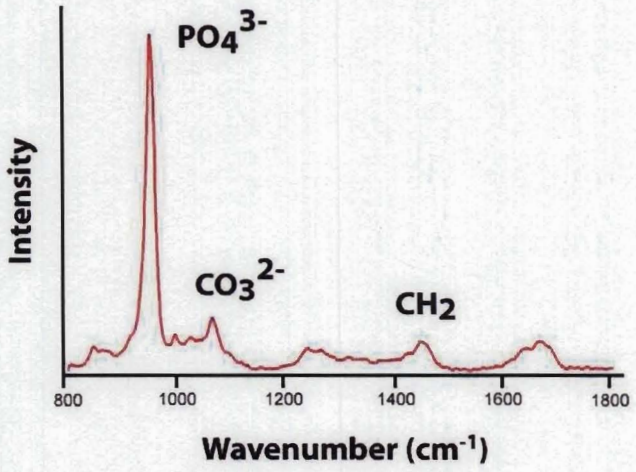

Figure 13. Typical Raman spectrum of cortical bone tissue in a mouse tibia. The phosphate (PO_4^{3-}), carbonate (CO_3^{2-}), and methylene (CH_2) peak heights are used to measure the mineral:matrix (PO_4^{3-}:CH_2) and carbonate substitution (CO_3^{2-}:PO_4^{3-}) ratios in bone. The phosphate, carbonate, and methylene peaks are located at approximately 961 cm^{-1}, 1068 cm^{-1}, and 1450 cm^{-1}, respectively.

For bone tissue, different methods have been employed to gain structural and material information. Fourier-transform infrared spectroscopy (FT-IR) has been a reliable method in evaluating the degree mineralization (expressed as mineral:matrix ratio) in cortical (dense) and trabecular (cancellous) bone[16,17]. Traditional IR, which measures vibrational motion, separates and detects emitted light energy by frequency. FT-IR simultaneously detects and measures all frequencies providing greater speed, sensitivity, and measurement accuracy than traditional IR[7]. The vibrational bands characteristic to bone mineral and the organic collagen matrix are distinguishable in the FT-IR wavenumber region (800-1800 cm^{-1}). Although FT-IR provides rapid spectral acquisition, sample preparation is time consuming as specimens must be, dehydrated, embedded, and cut into thin sections[6].

Raman spectroscopy has become a popular spectroscopic method to analyze bone tissue[6]. Based on the Raman effect, Raman spectroscopy measures the energy change associated with the reflectance of inelastically scattered light. When a photon-molecule collision occurs, a majority of the incident light scatters elastically and experiences an energy change of zero ($\Delta E=0$). A small percentage of light, however, will scatter inelastically and a shift in energy will occur ($\Delta E\neq 0$). Raman spectroscopy, like other forms of spectroscopy, accounts for shifts in energy which are unique to chemical specimens[21].

Providing high resolution at the micro-scale level, Raman spectroscopy is sensitive to specific bone tissue constituents. Phosphate (PO_4^{3-}), carbonate (CO_3^{2-}), and collagen methylene bonds (CH_2) are used to measure the degree of mineralization, expressed as the mineral:matrix ratio (PO_4^{3-}:CH_2), and the degree of type-B carbonate substitution for phosphate (CO_3^{2-}:PO_4^{3-}) in the mineral lattice. FT-IR and Raman bone studies use these ratios to assess cortical and trabecular bone composition[5,6,16]. Raman spectroscopy, however, offers advantages from FT-IR. Dehydration, embedding, and thin-sectioning of samples are not required since Raman spectroscopy operates in reflectance rather than in transmittance mode as used by FT-IR[6]. Sample preparation is thus minimal.

Several FT-IR and Raman studies have used the mineral:matrix and carbonate substitution ratios to assess bone material quality in aged and diseased bone[1,2,6,15,22,23,25]. With age, mineralization and carbonate substitution increased in mouse calvaria (skull) and with decreasing elastic deformation capacity in rat femora[1,22]. Increasing mineralization and carbonate substitution may increase bone fragility and deteriorate the

lattice symmetry, creating vacancies, which in turn have mechanical consequences[18]. In osteoporotic human bone, however, mineralization decreased while carbonate substitution increased relative to healthy bone[15]. These studies illustrate the fluctuation of material properties among different groups and that neither ratio solely assesses bone quality. Combined, these ratios provide information on tissue remodeling and the changing mineral lattice structure[15].

The effects of age and disease on bone quality have been widely addressed but the effects of mechanical loading and sex on composition in healthy bone have not been reported. Our study, for the first time, addressed the effects of *in vivo* mechanical loading and sex on bone tissue composition in the tibial cortices of mice. We also examined the effects of age and cortical location on composition and any interactions they may have with loading and sex. The degree of bone tissue mineralization (mineral:matrix) and carbonate substitution in the cortical tissue of mouse tibiae were assessed using Raman spectroscopy. We expected that *in vivo* mechanical loading, sex, age, but not cortical location would influence bone tissue composition. The purpose of this study was to test the hypothesis that mineralization at the periosteum decreases with loading[23]. We also tested the hypothesis that males and females differ in their material compositions[28].

Materials and Methods

Experimental Design

C57BL/6J male and female mice (Jackson Laboratories, Bar Harbor, ME) were received and acclimated to the Cornell Transgenic Mouse Core Facility. At the start of the experiment, 10 week old male and female (n=5/sex) and 6 month old female (n=5)

were caged in groups of up to four animals and fed ad libitum. The mouse model was chosen based on previous studies evaluating geometric changes with mechanical loading[11]. All experimental procedures were approved by the Institutional Animal Care and Use Committee.

Mechanical Loading Protocol

An axial compressive loading scheme was used in this experiment[11]. Compressive loads were applied by an electro-magnetic actuator (LA18-18-000A, BEI Kimco Magnetics, San Marcos, CA) to the left tibia while mice were under isoflurane anesthesia (0.8L/min, 2% isoflurane). The tibia was placed between two brass platens with the distal end (foot) connected to the actuator and the proximal end (knee) connected to a 100 N load cell (ELFS-T3E, Entran, Fairfield, NJ). The proximal plate was adjustable to fit different tibial lengths. Mice underwent 2 weeks (5 days/week, 1200 cycles/day) of cyclic compression at 4 Hz to induce loads of -11.5 N at the mid-diaphysis. The right tibia served as a contralateral control. After 2 weeks of loading, mice were euthanized by CO_2 inhalation. The left and right tibiae were dissected and stored in 70% ethanol before Raman spectral analysis.

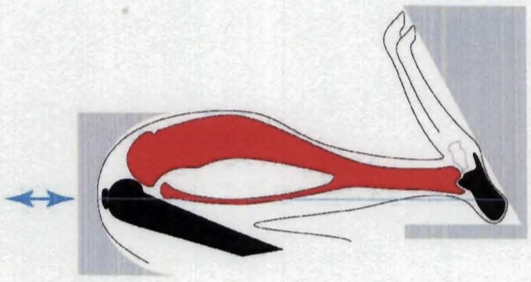

Figure 14. Schematic of tibial loading device. Arrows indicate the direction of axial compression. 11.5N were applied for 2 weeks (5 days/week) at 4 Hz for 1200 cycles/day.

Bone Tissue Composition Analysis

Each tibia was cut at the mid-diaphysis using a low-speed diamond saw (Isomet 1000 Buehler Ltd., Lake Bluff, Illinois). A custom jig was used to position the bone perpendicular to the saw blade (Appendix A). The exposed mid-diaphyseal cross section was positioned on an XY stage under an optical camera microscope. The periosteum of the lateral, medial, and posterior quadrants were examined in the 10 week old male and female and 6 month old female mice (Fig. 5). The periosteum was selected as loading was expected to induce new bone formation in this location. In the 6 month old females, spectra were also collected across the entire cortical thickness in the lateral, medial, and posterior quadrants to analyze cortical variation in mineral:matrix and carbonate substitution ratios (Fig.6). Spectra were collected over the 800-1800 cm^{-1} range using a 785 nm laser with a 50x, 0.75 N-A objective and a spatial resolution of 1 μm (Renishaw Inc. Gloucestershire, U.K.).

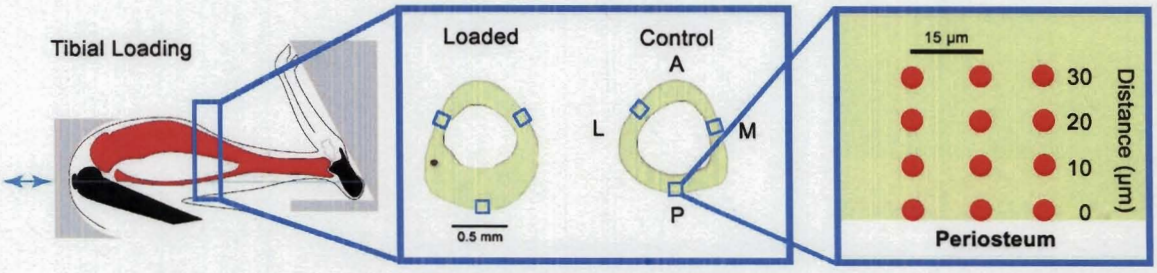

Figure 15. Schematic of tibial loading and compositional analysis protocols. The tibiae were cut at the mid-diaphysis to expose the lateral (L), medial (M), and posterior (P) quadrants. Twelve spectra (red dots) were taken in each quadrant. Four rows (3 spectra/row) were examined at 10 μm increments from the surface edge. The three spectra in each row were distanced 15 μm apart and treated as repeated measures.

At the periosteum, twelve spectra were collected in each quadrant. Four rows (3 spectra/row) were examined at 10 μm increments from the surface edge (Fig. 5). Across the entire cortical thickness, fifteen spectra were collected in each quadrant. Five rows (3

spectra/row) were collected at the periosteum (0%) to the endosteum (100%) with incremental rows at 25, 50, and 75% across the width of the cortex (Fig.6). The three spectra collected in each row were spaced 15 μm apart and treated as repeated measures. One spectral acquisition consisted of three scan accumulations (10 seconds/accumulation) for a total of 30 seconds/spectrum. Spectra were collected using Wire 2.0 software (Renishaw Inc., Gloucestershire, U.K.).

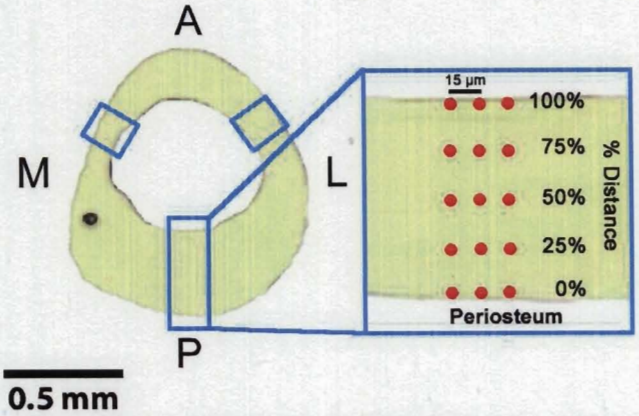

Figure 16. Schematic of Raman spectra collected in 6 month old female mice. Spectra taken across the entire cortex in the lateral (L), medial (M), and posterior (P) quadrants. Spectra (red dots) were collected at the periosteum (0%) to the endosteum (100%) and at 25, 50, and 75% across the width of the cortex.

Once collected, baseline corrections were made to each spectrum using a 3-factor polynomial and peak heights of the phosphate (957-962 cm^{-1}), carbonate (1065-1071 cm^{-1}), and collagen methylene (1447-1452 cm^{-1}) bands were determined using in-house MATLAB code (Simulink V7.0, The Mathworks). Mineral:matrix (PO_4^{3-}:CH_2) and Type-B carbonate substitution (CO_3^{2-}:PO_4^{3-}) ratios were calculated using the peak intensities of these bands to characterize material composition. For the 30 μm by 30 μm periosteal grid, the mineral:matrix and carbonate substitution ratios were averaged by limb (loaded vs. control) and by cortical location (quadrant) for all five animals in each group. Across the entire cortex, the mineral:matrix and carbonate substitution ratios were averaged at

each distance by limb and by cortical location. The effects of mechanical loading, sex, age, and cortical location were examined by a multi-factorial ANOVA and paired t-tests (Minitab Inc., State College, PA and JMP 6, SAS Institute Inc., Cary, NC). Data are reported as means ±SD. All statistical analyses are detailed in Appendix B.

Results

In vivo mechanical loading had a pronounced effect on the degree of mineralization at the periosteum. Following two weeks of loading, the mineral:matrix ratio was reduced in loaded relative to control limbs in all mouse groups (Fig. 7). Percent decreases in the mineral:matrix ratio with loading were not different across the three mouse groups (Fig. 8). The mineral:matrix ratio was reduced with loading in the lateral and medial quadrants of 10 week old females. 6 month old females experienced reduced mineralization with loading in the posterior quadrant (Fig 9). When viewed across the entire cortex in 6 month old females, the mineral:matrix ratio was reduced with loading at the periosteum and up to 25% of the width of the cortex (Fig. 10).

Sex, age, and cortical location influenced the degree of mineralization at the periosteum in the control limbs. By sex, the mineral:matrix ratio was greater in 10 week males than in 10 week females (Fig. 7). By age, the mineral:matrix ratio was greater in 6 month old females than in 10 week old females. Cortical location influenced the mineral:matrix ratio in 6 month old females with the posterior region having the most mineralized tissue (Fig. 9). Cortical location did not affect mineralization in 10 week old males and females.

Carbonate substitution in the control limbs was different between 10 week old males and females. Carbonate substitution was greater in females than in males (Fig. 7). Loading, age, and cortical location did not have an effect on carbonate substitution in any of the mouse groups. (Fig 7 & 9). Finally, carbonate substitution in the 6 month old females did not vary across the entire cortex in the loaded and control limbs (Fig. 10).

(A)

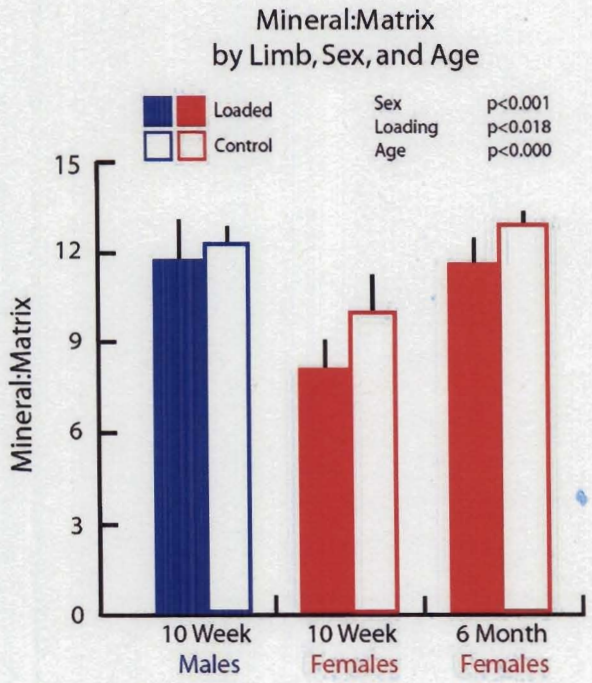

(B)

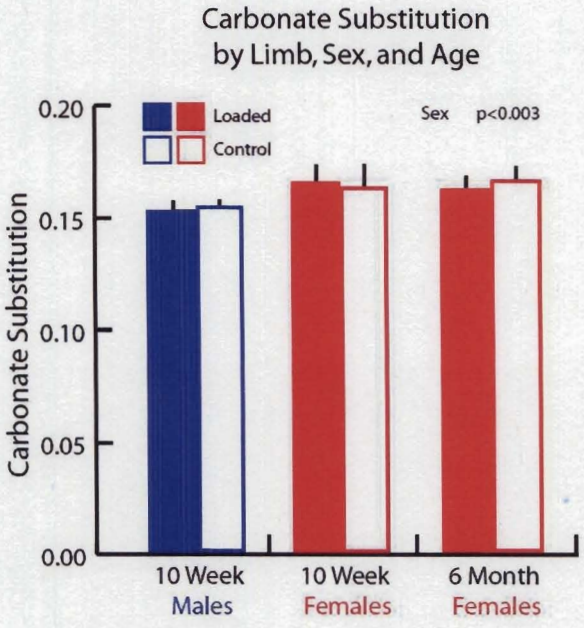

Figure 17. (A) Degree of mineralization, expressed as mineral:matrix ratios and (B) carbonate substitution in the loaded and control tibiae of 10 week old male and female and 6 month old female mice. Data represents mean ± SD for all three cortical location (n=5 animals/group). Significant effects listed above bars ($p<0.05$).

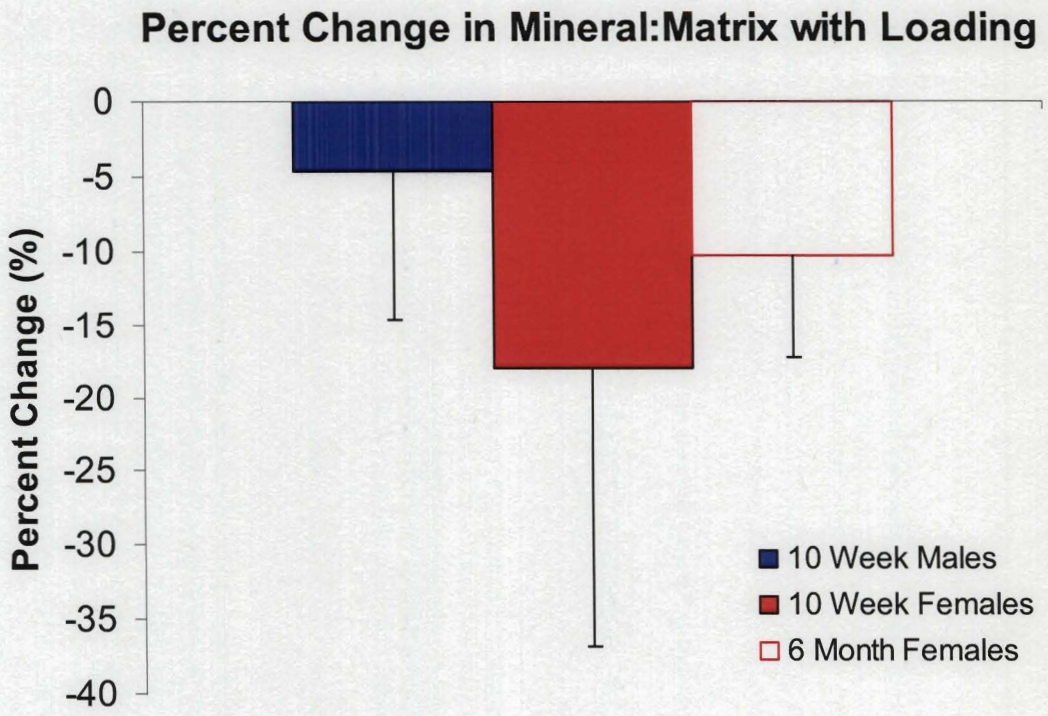

Figure 18. Relative percent change in mineral:matrix ratio in 10 week old male and female and 6 month old female mice. Percent change is calculated as [(Loaded-Control)/Control]*100%. Data represents mean ± SD for all three cortical location (n=5 animals/group).

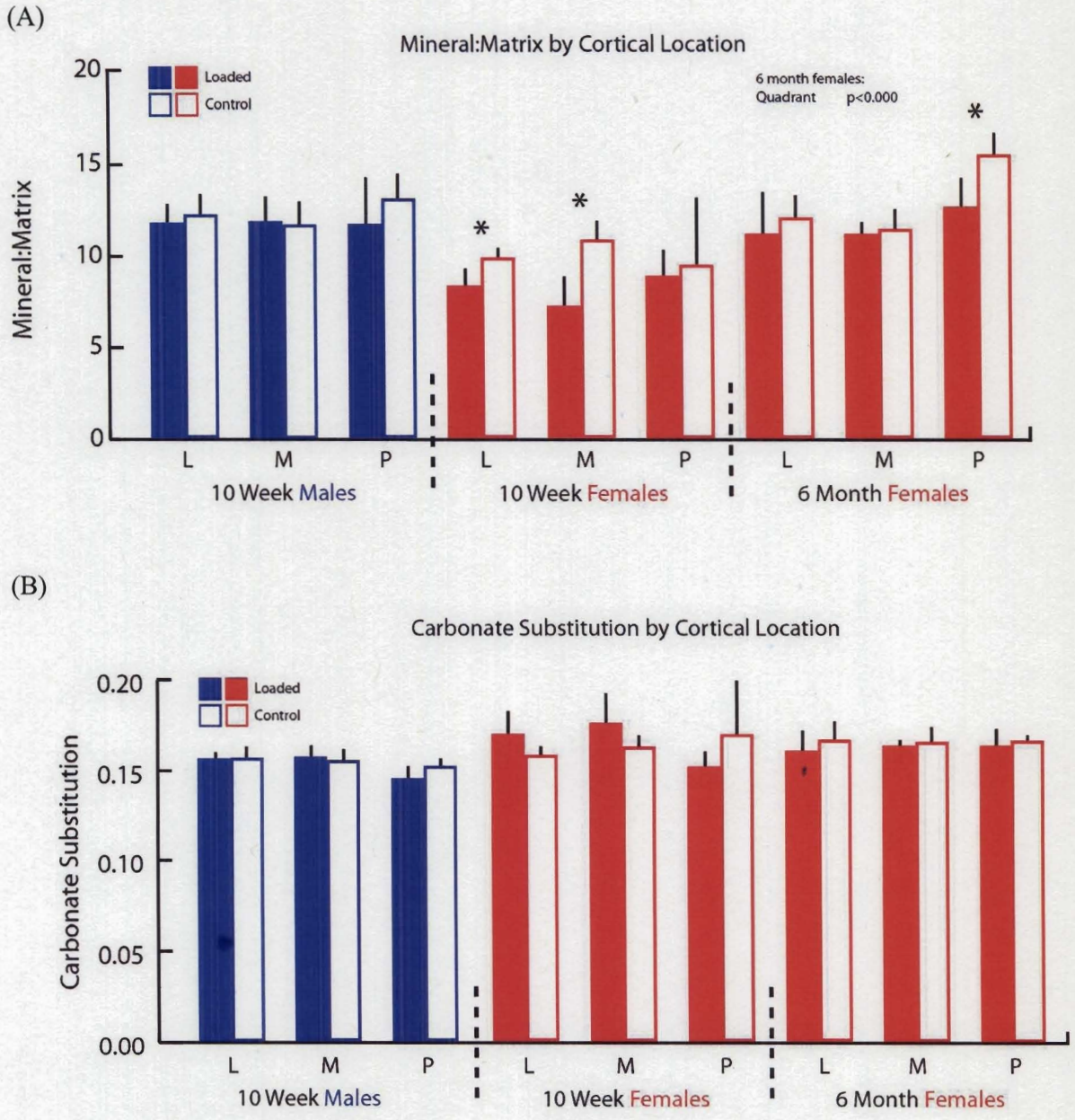

Figure 19. (A) Degree of mineralization, expressed as mineral:matrix ratios and (B) carbonate substitution in the loaded and control tibiae of 10 week old male and female and 6 month old female mice. Cortical location (quadrant) had and effect on mineralization in the control limbs of 6 month females ($p<0.000$). Data represents mean ± SD for the lateral (L), medial (M), and posterior (P) quadrants in n = 5 animals/group. *Indicates significant differences between loaded and control limbs ($p<0.05$).

(A)

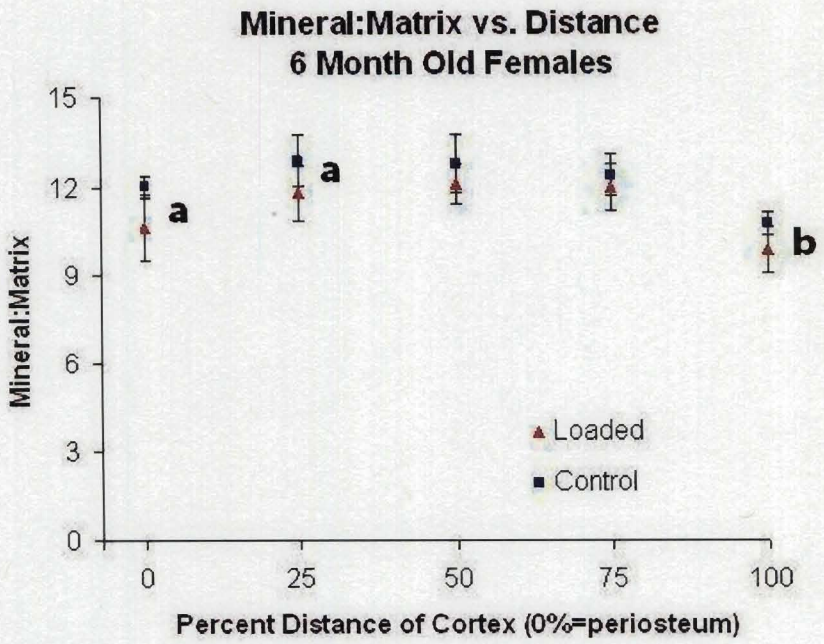

(B)

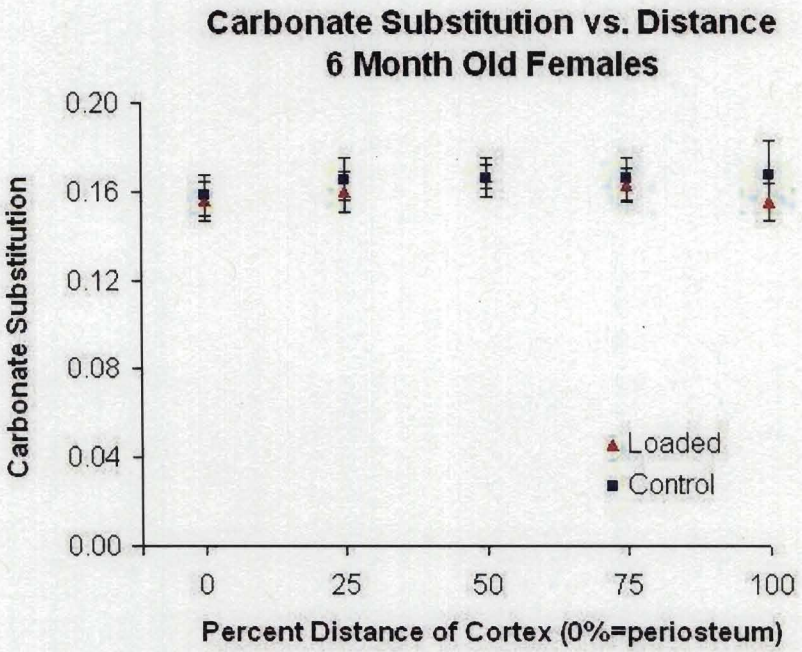

Figure 20. (A) Mineral:matrix and (B) carbonate substitution ratios for the loaded and control limbs as a percent of the average cortical distance from the periosteum (0%) to the endosteum (100%).

a Loaded limb significantly different from control limb.

b Control limb significantly different from all other control limbs ($p<0.05$).

See Appendix B for statistical table.

Discussion

We demonstrated that in a mouse model of noninvasive tibial loading the mineralization of periosteal tissue formed following loading was lower than contralateral limbs in both male and female mice and in growing and mature mice. The decreased mineralization in the loaded limbs reflects that loading induces new bone formation on the periosteum which is less mineralized than the pre-existing cortex. Furthermore, mineralization was reduced in the loaded relative to the control limbs from the periosteum to 25% of the width of the entire cortex in the mature 6 month females. Mineralization was fairly uniform between loaded and control limbs along the rest of the cortex indicating that, as expected, mechanical loading had the greatest influence at the periosteum. Carbonate substitution, on the other hand, did not respond to mechanical stimulus as the values between loaded and control limbs were similar.

Interestingly, the endosteal edge was less mineralized than other locations in the control limbs along the width of the cortex in the mature 6 month old female mice. Reduced mineral composition at the endosteum suggests the presence of younger bone relative to the rest of the cortex in the control limbs. Unfortunately, we did not examine the full width of the cortex in the tibia of growing mice. The mineralization gradient we measured across the cortex of mature female mice showed a gradient similar to IR measurements in the tibiae of 10 week old rats[5]. Carbonate substitution values remained uniform throughout the entire width of the cortex which was different from the increase in substitution with tissue age found in rats[9].

Sex differences in bone composition with loading have not been previously reported. Here, males had greater mineralization and lower carbonate substitution at the

periosteum than females (Fig.8). The sex-based difference in tissue composition may indicate that male mice had a more localized, smaller adaptive response to loading, or, alternatively, more rapid mineralization of newly formed tissue compared to female mice. These compositional differences may contribute to sex-based differences in whole bone mechanical properties[1,9,28].

Mineralization increased with age in our female samples. Growing 10 week old female mice had substantially less mature bone tissue than 6 month old female mice. Increased mineral deposition has been reported for mouse tibiae[1,22]. Surprisingly, carbonate substitution was not affected by age in the mouse tibia. Carbonate substitution has previously been reported to increase with age in rat femora and mouse calvaria[1,22] and to decrease with age in human osteonal tissue[16]. The different effects of age on carbonate substitution may be related to the species, the type of bone tissue examined, or the measurement technique.

Finally, cortical location affected mineralization, but not carbonate substitution, in mature (6 month old) females. Mineralization and carbonate substitution did not vary by quadrant in either growing group, consistent with findings reported previously for the femora of 9 week old Swiss-Webster mice[20]. Increased mineralization was present, however, in the posterior quadrant of the tibia from mature female mice. Cortical tissue from mature mice that are no longer actively forming bone may be more homogeneous locally. Greater variability was present in compositional measurements from cortical tissue of both growing animals and loaded limbs in mature mice. Therefore, we were only able to measure quadrant-based differences in mature female cortices.

Interpretation of our bone composition results is affected by strengths and limitations of our experimental design. *In vivo* loading of the mouse tibia repeatedly induces geometric changes through bone formation in growing mice and inhibition of bone loss in hormone-deficient mice[29]. The effects of *in vivo* loading on bone tissue composition have not been reported previously, nor have these effects been examined as a function of age, sex, and cortical location. However, our approach did have several limitations in the study design and measurements. First, we characterized material changes through chemical composition and did not include other measures of bone mass and structure. Therefore, we could not correlate geometric or mechanical changes to the material composition. Second, to fully appreciate the effects of sex and age on cortical composition, a complete experimental design would require data from mature male mice following *in vivo* loading in addition to the female and growing male data reported here. Finally, compositional measures obtained from Raman spectra have not been validated by more standard metrics such as ash weight as is the case for FT-IR spectroscopy[30].

In conclusion, we have shown that loading, sex, age, and cortical location influence material properties in mouse tibiae. Mechanical loading stimulates bone growth which may provide non-pharmacological approaches toward improving bone quality. Material composition varies by sex, age, and other factors which must be taken into consideration when developing a protocol to stimulate new bone growth. Combining geometric, mechanical, and material information will provide researchers and physicians with a more complete view of whole bone function.

References

1. Akkus O, Adar F, Schaffler MB 2004 Age-related changes in physicochemical properties of mineral crystals are related to impaired mechanical function of cortical bone. Bone **34**(3):443-453.

2. Akkus O, Polyakova-Akkus A, Adar F, Schaffler MB 2003 Aging of Microstructural Compartments in Human Compact Bone. Journal of Bone and Mineral Research **18**(6):1012-1019.

3. Boskey AL, Wright TM, Blank RD 1999 Collagen and Bone Strength. Journal of Bone and Mineral Research **14**(3):330-335.

4. Burstein AH 2001 Basic Biomechanics of the Musculoskeletal System. 3rd ed. J Bone Joint Surg Am **83**(9):1455.

5. Busa B, Miller L, Rubin C, Qin YX, Judex S 2005 Rapid Establishment of Chemical and Mechanical Properties during Lamellar Bone Formation. Calcified Tissue International **77**(6):386-394.

6. Carden A, Morris MD 2000 Application of vibrational spectroscopy to the study of mineralized tissues (review). Journal of Biomedical Optics **5**(3):259-268.

7. Chang R 2000 Physical Chemistry for the Chemical and Biological Sciences, 3rd ed. University Science Books, pp 1010.

8. Ding M, Dalstra M, Linde F, Hvid I 1998 Mechanical properties of the normal human tibial cartilage-bone complex in relation to age. Clinical Biomechanics **13**(4-5):351-358.

9. Donnelly E, Boskey, A.L., Baker, S.P., van der Meulen M.C.H. 2009 Effects of tissue age on bone tissue material composition and nanomechanical properties in the rat cortex. Journal of Biomedical Materials Research

10. Freeman JJ, Wopenka B, Silva MJ, Pasteris JD 2001 Raman Spectroscopic Detection of Changes in Bioapatite in Mouse Femora as a Function of Age and In Vitro Fluoride Treatment. Calcified Tissue International **68**(3):156-162.

11. Fritton JC, Myers ER, Wright TM, van der Meulen MCH 2005 Loading induces site-specific increases in mineral content assessed by microcomputed tomography of the mouse tibia. Bone **36**(6):1030-1038.

12. Lanyon 1979 The relationship of functional stress and strain to the processes of bone remodelling. An experimental study on the sheep radius. biomechanics **12**(8):593.

13. Main RP, et al. 2008 Tibial strains decrease following *in vivo* loading In female not male mice ORS.

14. Martin RB 2003 Bones: structure and mechanics: John D. Currey (Ed.), Princeton University Press, Princeton, NJ. Journal of Biomechanics **36**(6):893-893.

15. McCreadie BR, Morris MD, Chen T-c, Sudhaker Rao D, Finney WF, Widjaja E, Goldstein SA 2006 Bone tissue compositional differences in women with and without osteoporotic fracture. Bone **39**(6):1190-1195.

16. Paschalis EP, DiCarlo E, Betts F, Sherman P, Mendelsohn R, Boskey AL 1996 FTIR Microspectroscopic Analysis of Human Osteonal Bone. Calcified Tissue International **59**(6):480-487.

17. Paschalis EP, Verdelis K, Doty SB, Boskey AL, Mendelsohn R, Yamauchi M 2001 Spectroscopic Characterization of Collagen Cross-Links in Bone. Journal of Bone and Mineral Research **16**(10):1821-1828.

18. Penel G, Leroy G, Rey C, Bres E 1998 MicroRaman Spectral Study of the PO4 and CO3 Vibrational Modes in Synthetic and Biological Apatites. Calcified Tissue International **63**(6):475-481.

19. Porter A, Patel N, Brooks R, Best S, Rushton N, Bonfield W 2005 Effect of carbonate substitution on the ultrastructural characteristics of hydroxyapatite implants. Journal of Materials Science: Materials in Medicine **16**(10):899-907.

20. Ramasamy JG, Akkus O 2007 Local variations in the micromechanical properties of mouse femur: The involvement of collagen fiber orientation and mineralization. Journal of Biomechanics **40**(4):910-918.

21. Renishaw I Introduction to Raman Spectroscopy. Renishaw, Inc., Gloucestershire, UK

22. Tarnowski CP, Ignelzi MA, Morris MD 2002 Mineralization of Developing Mouse Calvaria as Revealed by Raman Microspectroscopy. Journal of Bone and Mineral Research **17**(6):1118-1126.

23. Tarnowski CP, Ignelzi MA, Wang WEI, Taboas JM, Goldstein SA, Morris MD 2004 Earliest Mineral and Matrix Changes in Force-Induced Musculoskeletal Disease as Revealed by Raman Microspectroscopic Imaging. Journal of Bone and Mineral Research **19**(1):64-71.

24. Thurner PJ, Erickson B, Jungmann R, Schriock Z, Weaver JC, Fantner GE, Schitter G, Morse DE, Hansma PK 2007 High-speed photography of compressed human trabecular bone correlates whitening to microscopic damage. Engineering Fracture Mechanics **74**(12):1928-1941.

25. van Apeldoorn AA, de Boer J, van Steeg H, Hoeijmakers JHJ, Otto C, van Blitterswijk CA 2007 Physicochemical Composition of Osteoporotic Bone in the Trichothiodystrophy Premature Aging Mouse Determined by Confocal Raman Microscopy. J Gerontol A Biol Sci Med Sci **62**(1):34-40.

26. van der Meulen MCH, Jepsen KJ, Mikic B 2001 Understanding bone strength: size isn't everything. Bone **29**(2):101-104.

27. Whitesides TE 2001 Orthopaedic Basic Science. Biology and Biomechanics of the Musculoskeletal System. 2nd ed. J Bone Joint Surg Am **83**(3):481.

28. Wu X-P, Yang Y-H, Zhang H, Yuan L-Q, Luo X-H, Cao X-Z, Liao E-Y 2005 Gender differences in bone density at different skeletal sites of acquisition with age in Chinese children and adolescents. Journal of Bone and Mineral Metabolism **23**(3):253-260.

29. Fritton JC, Myers ER, Wright TM, van der Meulen MC 2008 Bone mass is preserved and cancellous architecture altered due to cyclic loading of the mouse tibia after orchidectomy. Journal of Bone and Mineral Research **23**(5):663-71.

30. Boskey A, Mendelsohn R 2005 Infrared analysis of bone in health and disease. Journal of Biomedical Optics **10**(3):031102.

Appendix A

Methods and Materials Images

(A)

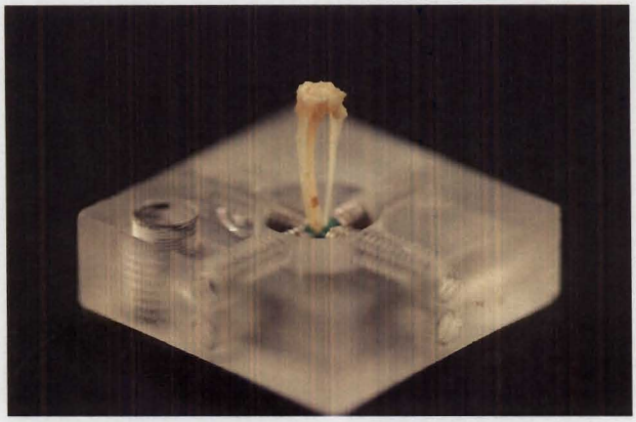

(B)

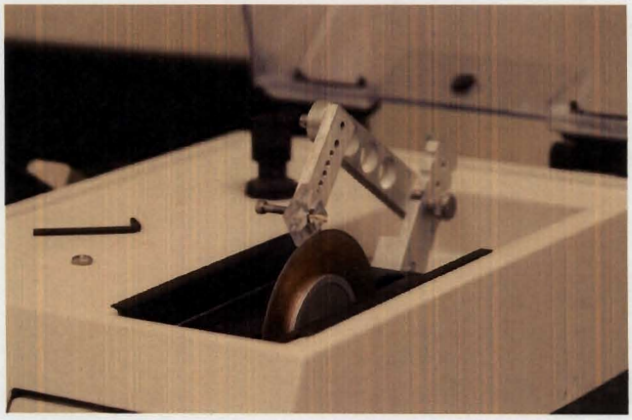

(C)

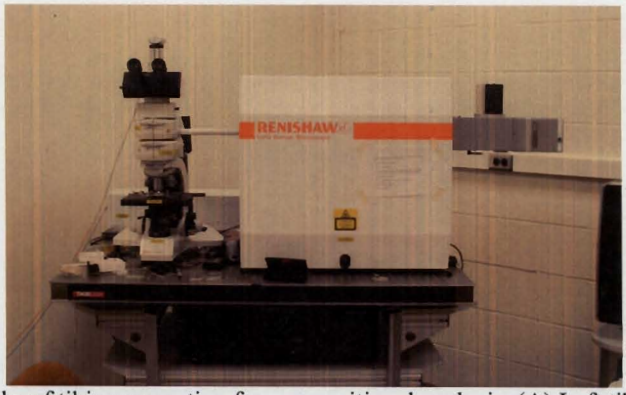

Figure A21. Photographs of tibia preparation for compositional analysis. (A) Left tibia positioned in custom jig. (B) Tibial mid-diaphysis positioned perpendicular to diamond blade saw. (C) 785 nm Raman laser with optical microscope.

Appendix B

Mineral:Matrix and Carbonate Substitution Table

Table I. Mineral:Matrix and Carbonate Substitution values for all mouse groups examined. Data represents mean ± SD

	10 Week Males		10 Week Females		6 Month Females	
	Loaded	Control	Loaded	Control	Loaded	Control
Mineral:Matrix	11.6 ± 1.3	12.2 ± 0.5	7.9 ± 1.0	9.9 ± 1.2	11.5 ± 0.8	12.8 ± 0.4
Carb. Subst.	0.151 ± 0.005	0.153 ± 0.003	0.164 ± 0.008	0.162 ± 0.010	0.161 ± 0.006	0.165 ± 0.006

Statistical Tests

Table II. ANOVA results comparing the mean of loaded limb against the control limb at a % distance in 6 month old female mice. ***Indicates** loaded limb significantly lower than the control ($p<0.05$). Table supplements Figure 22.

	Periosteum				Endosteum
% Distance	0	25	50	75	100
Mineral:Matrix	**p<0.0430***	**p=0.0382***	p=0.3253	p=0.4789	p=0.0794
Carbonate Substitution	p=0.5918	p=0.4393	p=0.9134	p=0.6591	p=0.1658

Appendix C

Sample Data Table

Table shows the average peak intensity, mineral:matrix, and carbonate substitution values for the entire data set (1080 rows of data) by animal and limb. See Figure 23 for graphical summary.

CODE: Animal

CODE	SEX	AGE	BONE	PO_4^{3-}	CH_2	CO_3^{2-}	PO_4^{3-}:CH_2	CO_3^{2-}:PO_4^{3-}
A03	F	10	L	5555	747	851	7.68	0.154
A03	F	10	C	6385	642	994	10.37	0.157
A05	F	26	L	15100	1367	2429	11.25	0.161
A05	F	26	C	12936	1028	2130	12.76	0.165
B07	F	26	L	11362	1118	1834	10.19	0.157
B07	F	26	C	16051	1263	2774	13.01	0.174
B08	F	10	L	6861	745	1107	9.47	0.161
B08	F	10	C	5864	722	926	8.46	0.159
C10	F	10	L	6127	830	1022	7.72	0.168
C10	F	10	C	7299	943	1317	8.75	0.180
D13	F	10	L	5421	812	918	6.83	0.174
D13	F	10	C	6913	669	1101	10.43	0.159
E19	F	10	L	6342	807	1045	7.96	0.164
E19	F	10	C	6686	619	1037	11.35	0.155
F03	M	10	L	6507	554	990	11.84	0.153
F03	M	10	C	6179	547	936	11.48	0.151
G07	M	10	L	7112	620	1106	11.54	0.156
G07	M	10	C	6041	502	920	12.14	0.152
G12	F	26	L	14188	1134	2416	12.42	0.170
G12	F	26	C	14441	1108	2423	13.46	0.168
G14	F	26	L	14359	1224	2312	11.71	0.162
G14	F	26	C	15513	1301	2470	12.49	0.159
H10	M	10	L	5499	641	834	9.45	0.153
H10	M	10	C	6668	565	1028	12.06	0.155
H17	F	26	L	14438	1234	2244	11.86	0.155
H17	F	26	C	14738	1196	2337	12.38	0.159
I15	M	10	L	6653	534	963	12.64	0.144
I15	M	10	C	6727	561	1051	12.35	0.157
J18	M	10	L	6328	502	950	12.72	0.150
J18	M	10	C	6450	509	972	12.95	0.151